JOC Article

Alkanethioimidoyl Radicals: Evaluation of β-Scission Rates and of Cyclization onto *S*-Alkenyl Substituents

Matteo Minozzi,[†] Daniele Nanni,*[,†] and John C. Walton*[,‡]

School of Chemistry, University of St. Andrews, Fife, KY16 9ST, United Kingdom, and Dipartimento di Chimica Organica "A. Mangini", Università di Bologna, Viale Risorgimento 4, I-40136 Bologna, Italy

jcw@st-andrews.ac.uk

Received September 16, 2003

Thioimidoyl radicals were generated by addition of alkylsulfanyl radicals to alkyl isonitriles and were characterized by electron paramagnetic resonance (EPR) spectroscopy. The β-scissions of their C•S−C bonds were studied by variable-temperature EPR spectroscopy and the fragmentation rate constants and activation energies were calculated. The scission rates depend on the stability of the released alkyl radicals but in any case, at room temperature, the processes were fast. Data collected on similar oxyimidoyls showed that their fragmentations are slightly slower compared to those of analogous thioimidoyls. The scission rates of selenoimidoyls could not be studied by EPR and were evaluated by theoretical calculations. EPR experiments also enabled both β-scission and *5-exo* ring closure rate constants of two *S*-but-3-enyl-substituted imidoyl radicals to be determined, showing that cyclization prevails only at low temperatures. Density functional theory (DFT) theoretical calculations predicted that the fragmentation process preferentially occurs from the *s-cis* rotamers (X−C bond) of the imidoyl radicals. Thio- and seleno-imidoyls (but not oxyimidoyls) prefer *s-trans* conformations so that their fragmentations involve prior rotation about the X−C bond.

Introduction

Imidoyl radicals ($R^1N{=}C^{\bullet}R^2$) are finding increasing use as synthetic intermediates, especially since the discovery of several stylish annulations based around their formation from imines or isonitriles and subsequent cyclizations to give quinolines, cyclopentaquinolines, and related heterocycles.[1−3] Thioimidoyl radicals ($R^1N{=}C^{\bullet}SR^2$) can be made from sulfanyl radical additions to isonitriles[3] or by aryl radical additions to isothiocyanates. The electron paramagnetic resonance (EPR) spectra of three archetype thioimidoyl radicals (R^1 = *t*-Bu; R^2 = Me, CF_3, and *t*-Bu) were briefly described by Blum and Roberts[4] in 1978. Recently, important cyclization and cascade sequences involving thioimidoyl radicals have been developed. For example, Bachi et al.[5] exploited ring closures of thioimidoyl radicals onto unsaturated *N*-substituents (R^1 = alkenyl) for the preparation of a variety of heterocycles, including kainic acid. Useful cascade sequences leading to benzothienoquinoxalines[6a] and -quinolines[6b] and thiochromenoindoles[7] have also been discovered.

SCHEME 1

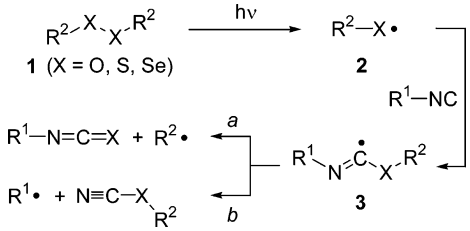

Two β-scission modes are available to α-heteroatom-substituted imidoyl radicals (Scheme 1). Scission of the X−R^2 bond (mode a) will give an isocyanate (isothiocyanate, isoselenocyanate) and C-centered radical $R^{2\bullet}$. Alternatively, scission of the R^1−N bond will give C-centered radical $R^{1\bullet}$ and a cyanate (thiocyanate, selenocyanate) (mode b).

Knowledge of the mechanistic details of thioimidoyl radical reactions and of the way β-scission rate constants respond to variations in the attached groups would be useful input for various aspects of synthetic design. For example, ring closure of a thioimidoyl radical **3** (X = S) onto an *S*-alkenyl substituent had not been reported prior to this work but appeared possible, provided the β-scis-

[†] University of Bologna.
[‡] University of St. Andrews.

(1) (a) Leardini, R.; Pedulli, G. F.; Tundo, A.; Zanardi, G. *J. Chem. Soc., Chem. Commun.* **1984**, 1320. (b) Leardini, R.; Nanni, D.; Pedulli, G. F.; Tundo, A.; Zanardi, G. *J. Chem. Soc., Perkin Trans. 1* **1986**, 1591.

(2) (a) Curran, D. P.; Liu, H. *J. Am. Chem. Soc.* **1991**, *113*, 2127. (b) Ryu, I.; Sonoda, N.; Curran, D. P. *Chem. Rev.* **1996**, *96*, 177. (c) Josien, H.; Ko, S.-B.; Bom, D.; Curran, D. P. *Chem. Eur. J.* **1998**, *4*, 67.

(3) For a review on radical addition to isonitriles, see Nanni, D. In *Radicals in Organic Synthesis*, Renaud, P., Sibi, M. P., Eds., Wiley−VCH: Weinheim, Germany, 2001; Vol. 2, Chapt. 1.3.1, pp 44−61.

(4) (a) Blum, P. M.; Roberts, B. P. *J. Chem. Soc., Chem. Commun.* **1976**, 535. (b) Blum, P. M.; Roberts, B. P. *J. Chem. Soc., Perkin Trans. 1* **1978**, 1313.

(5) (a) Bachi, M. D.; Balanov, A.; Bar-Ner, N. *J. Org. Chem.* **1994**, *59*, 7752. (b) Bachi, M. D.; Melman, A. *Synlett* **1996**, 60. (c) Bachi, M. D.; Melman, A. *J. Org. Chem.* **1997**, *62*, 1896. (d) Bachi, M. D.; Melman, A. *Pure Appl. Chem.* **1998**, *70*, 259.

(6) (a) Leardini, R.; Nanni, D.; Pareschi, P.; Tundo, A.; Zanardi, G. *J. Org. Chem.* **1997**, *62*, 8394. (b) Benati, L.; Leardini, R.; Minozzi, M.; Nanni, D.; Spagnolo, P.; Zanardi, G. *J. Org. Chem.* **2000**, *65*, 8669.

(7) Benati, L.; Calestani, G.; Leardini, R.; Minozzi, M.; Nanni, D.; Spagnolo, P.; Strazzari, S.; Zanardi, G. *J. Org. Chem.* **2003**, *68*, 3454.

10.1021/jo0353637 CCC: $27.50
Published on Web 02/19/2004

SCHEME 2 [a]

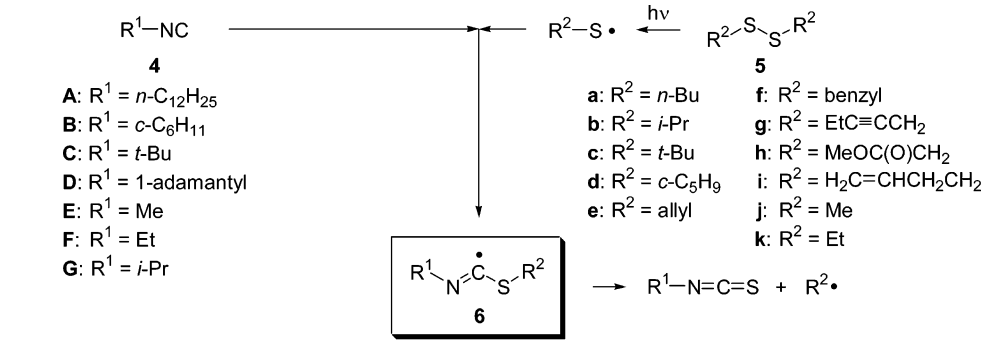

Aa: R^1 = *n*-$C_{12}H_{25}$, R^2 = *n*-Bu
Ab: R^1 = *n*-$C_{12}H_{25}$, R^2 = *i*-Pr
Ac: R^1 = *n*-$C_{12}H_{25}$, R^2 = *t*-Bu
Ad: R^1 = *n*-$C_{12}H_{25}$, R^2 = *c*-C_5H_9
Ba: R^1 = *c*-C_6H_{11}, R^2 = *n*Bu
Bb: R^1 = *c*-C_6H_{11}, R^2 = *i*-Pr
Bc: R^1 = *c*-C_6H_{11}, R^2 = *t*-Bu
Ca: R^1 = *t*-Bu, R^2 = *n*-Bu
Cb: R^1 = *t*-Bu, R^2 = *i*-Pr
Cc: R^1 = *t*-Bu, R^2 = *t*-Bu
Cd: R^1 = *t*-Bu, R^2 = *c*-C_5H_9
Ce: R^1 = *t*-Bu, R^2 = allyl
Cf: R^1 = *t*-Bu, R^2 = benzyl
Cg: R^1 = *t*-Bu, R^2 = EtC≡CCH_2
Ch: R^1 = *t*-Bu, R^2 = $MeOC(O)CH_2$
Ci: R^1 = *t*-Bu, R^2 = but-3-enyl
Da: R^1 = 1-adamantyl, R^2 = *n*-Bu
Db: R^1 = 1-adamantyl, R^2 = *i*-Pr
Dc: R^1 = 1-adamantyl, R^2 = *t*-Bu
Dd: R^1 = 1-adamantyl, R^2 = *c*-C_5H_9
Di: R^1 = 1-adamantyl, R^2 = but-3-enyl
Ej: R^1 = Me, R^2 = Me
Fk: R^1 = Et, R^2 = Et
Gb: R^1 = *i*-Pr, R^2 = *i*-Pr

[a] For clearness' sake, thioimidoyl radicals **6** are identified by both a capital letter (the *N*-substituent derived from the isonitrile) and a small letter (the *S*-substituent derived from the disulfide).

sion reactions were not too fast. We report in this paper our characterization of a representative range of thioimidoyl radicals and of their fragmentation rate constants, mainly by EPR spectroscopy, supplemented by end product analyses and by density functional theory (DFT) computations. For comparison purposes, several model oxyimidoyl (**3**, X = O) and selenoimidoyl radicals (**3**, X = Se) were examined by similar methods. On the basis of the measured fragmentation rates, it appeared that ring closure onto an *S*-alkenyl group might be observable and our study of the regiochemistry and rate of this process is also reported. Part of this research was published as a preliminary letter.[8]

Results and Discussion

Thioimidoyl radicals have previously been generated by addition of C-centered radicals to the *S*-atoms of isothiocyanates.[6,7,9] However, when a cyclopropane solution of acetyl peroxide and *n*-butyl isothiocyanate was photolyzed in the resonant cavity of an EPR spectrometer, only the methyl radical was observed in the whole temperature range (150−250 K).

In subsequent spectroscopic work, thioimidoyl radicals were generated exclusively by photolysis of a dialkyl disulfide (**5a**−**i**) in the presence of an alkane isonitrile (**4A**−**D**), and series of both substrates were prepared for this purpose by literature methods or adaptations thereof (Scheme 2).

EPR Spectra of Thioimidoyl Radicals. When a cyclopropane solution (ca. 0.2 mL) containing **4C** (10 mg) and **5c** (10 mg) in a quartz tube was photolyzed at 150 K with light from a 500 W Hg arc lamp in the resonant cavity of an EPR spectrometer, a three-line spectrum with EPR parameters characteristic of the thioimidoyl radical **6Cc** was observed (Figure 1 and Table 1). Figure 1 illustrates the striking difference in the appearance of an archetype thioimidoyl radical spectrum as compared with oxyimidoyl counterparts (see Supporting Information for the latter). At higher temperatures the spectrum of **6Cc** weakened and the spectrum of the *tert*-butyl radical appeared and became stronger as the temperature was raised. Above ca. 200 K only the *tert*-butyl radical could be detected.

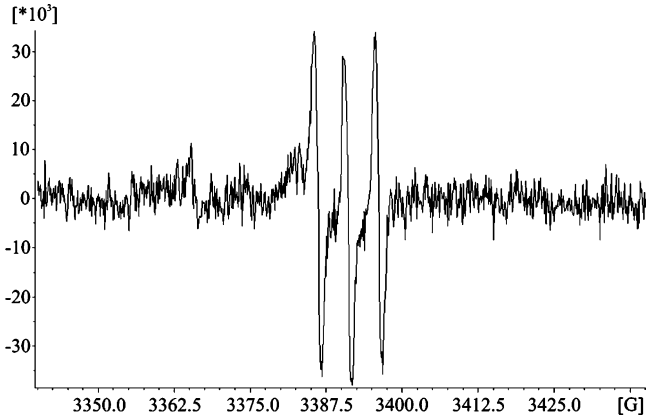

FIGURE 1. EPR spectrum of thioimidoyl radical **6Cc** at 150 K in cyclopropane.

Similar spectra of alkane thioimidoyl radicals **6** were observed for isonitriles **4A**−**D** with disulfides **5a**−**d**. Attempts were also made to observe arenethioimidoyl radicals by photolysis of diphenyl disulfide and other diaryl disulfides, together with alkyl isonitriles. However, no EPR spectra were obtained from these systems, probably because of the insolubility of these disulfides in cyclopropane. Hyperfine splittings (hfs) from H atoms of the *N*-substituents of **6** were resolved (see Figure 1) but hfs from H atoms of the *S*-substituents were not resolved in any case. The measured *g*-factors were all in the range 2.0008−2.0014 (Table 1) and are characteristic of oxyimidoyl and thioimidoyl radicals.[4] The low *g*-factors

(8) Minozzi, M.; Nanni, D.; Walton, J. C. *Org. Lett.* **2003**, *5*, 901.
(9) Barton, D. H. R.; Jaszberenyi, J. Cs.; Theodorakis, E. A. *Tetrahedron* **1992**, *48*, 2613.

TABLE 1. Experimental EPR Parameters for Thioimidoyl and Related Radicals[a]

	radical	*T*/K	*g*-factor	*a*(N)	*a*(H_β)
6Aa	*n*-$C_{12}H_{25}N{=}C^{\bullet}S$-*n*-Bu	255[a]	2.0011	4.12	1.98 (2H)
6Ab	*n*-$C_{12}H_{25}N{=}C^{\bullet}S$-*i*-Pr	170[a]	2.0008	4.43	1.96 (2H)
6Ad	*n*-$C_{12}H_{25}N{=}C^{\bullet}S$-*c*-$C_5H_9$	185[a]	2.0008	4.43	1.86 (2H)
6Ac	*n*-$C_{12}H_{25}N{=}C^{\bullet}S$-*t*-Bu	160[a]	2.0011	4.64	1.86 (2H)
6Ba	*c*-$C_6H_{11}N{=}C^{\bullet}S$-*n*-Bu	245[a]	2.0010	4.4	2.20 (1H)
6Bb	*c*-$C_6H_{11}N{=}C^{\bullet}S$-*i*-Pr	160[a]	2.0008	4.64	2.20 (1H)
6Bc	*c*-$C_6H_{11}N{=}C^{\bullet}S$-*t*-Bu	160[a]	2.0011	4.69	2.22 (1H)
6Ca	*t*-Bu$N{=}C^{\bullet}S$-*n*-Bu	255[a]	2.0012	4.58	
		210[b]	2.0011	4.70	
6Ci	*t*-Bu$N{=}C^{\bullet}S$-but-3-enyl	235[a]	2.0011	4.58	
6Cb	*t*-Bu$N{=}C^{\bullet}S$-*i*-Pr	150[a]	2.0009	4.83	
6Cd	*t*-Bu$N{=}C^{\bullet}S$-*c*-C_5H_9	215[a]	2.0009	4.74	
6Cc	*t*-Bu$N{=}C^{\bullet}S$-*t*-Bu	188	2.0014[c]	5.0	
		150[a]	2.0011	5.1	
6Da	Ad$N{=}C^{\bullet}S$-*n*-Bu	230[a]	2.0011	4.58	
6Di	Ad$N{=}C^{\bullet}S$-but-3-enyl	245[a]	2.0012	4.5	
6Db	Ad$N{=}C^{\bullet}S$-*i*-Pr	210[a]	2.0009	4.80	
6Dd	Ad$N{=}C^{\bullet}S$-*c*-C_5H_9	180[a]	2.0008	4.85	
6Dc	Ad$N{=}C^{\bullet}S$-*t*-Bu	175[a]	2.0013	5.10	
	n-$C_{12}H_{25}N{=}C^{\bullet}O$-*t*-Bu	205[a]	2.0014	≤0.7	1.36 (2H)
	c-$C_6H_{11}N{=}C^{\bullet}O$-*t*-Bu	220[a]	2.0014	≤0.7	2.01 (1H)
	t-Bu$N{=}C^{\bullet}O$-*t*-Bu		2.0016[c]	≤0.3	

[a] All hyperfine splitting values are in gauss; solvent = cyclopropane; Ad = 1-adamantyl. [b] Solvent = *tert*-butylbenzene. [c] See ref 4.

FIGURE 2. Resonance stabilization in imidoyl radicals.

and other EPR parameters are consistent with the idea that thioimidoyls are σ-radicals as suggested previously.[4,10,11]

Imidoyl radicals normally exhibit low *a*(N) values (1.2−1.9 G) that have been accounted for by a spin polarization mechanism that induces negative spin density at the *N*-atom, somewhat balancing the positive spin density resulting from resonance (Figure 2).

In thioimidoyl radicals, the ability of the *S*-atom to stabilize an α-negative charge[4] should increase the contribution of the right-hand canonical structure of Figure 2. This brings greater positive spin density onto the *N*-atom and hence accounts for the somewhat higher *a*(N) values (4.1−5.1 G) found for thioimidoyls (Table 1). It should be noted that, for each series of **6**, *a*(N) increases as the extent of branching at the α-C-atom of the *S*-alkyl substituent increases. Several oxyimidoyl radicals, generated by photolysis of di-*tert*-butyl peroxide (DTBP) and an isonitrile, were also observed and their EPR parameters are included in Table 1.

For all the radicals **6Aa**−**6Dd** the EPR spectra at higher temperatures showed mainly the C-centered radical $R^{2\bullet}$ with hfs identical to those given in the literature.[12] That $R^{2\bullet}$ was released (by C−S bond scission) and *not*

SCHEME 3

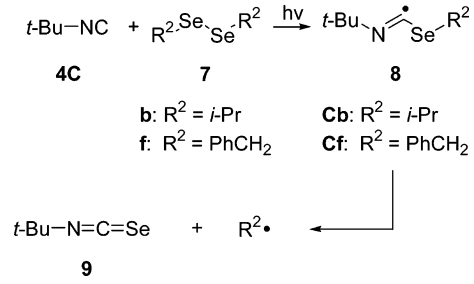

$R^{1\bullet}$ was confirmed by the unsymmetrical thioimidoyls, none of which showed any trace of $R^{1\bullet}$. GC−MS analyses of the reaction products provided further evidence that β-scission took place exclusively by fragmentation of the $S{-}R^2$ bond.[13] In each case *only* the isothiocyanate $R^1{-}N{=}C{=}S$ was detected, not the alternative thiocyanate $NCS{-}R^2$.

Photolyses were also carried out with disulfides **5e**−**h** and *tert*-butyl isonitrile **4C**. In each case the corresponding thioimidoyl radical was *not* detected, even at the lowest accessible temperature (ca. 120 K in *n*-propane solvent). Instead the allyl, benzyl, pent-2-ynyl, or (methoxycarbonyl)methyl radical was observed. Evidently, the rate of the β-scission process was enhanced by the resonance stabilization in the released radical.

A search for selenoimidoyl radicals **8** was carried out by photolysis of **4C** with dibenzyl diselenide **7f** (Scheme 3). EPR spectroscopy showed only the benzyl radical down to 150 K in cyclopropane solvent.[14] GC−MS analysis of the reaction mixture established that the main products were *tert*-butyl isoselenocyanate **9** and dibenzyl (the latter to a major extent). This suggested that, at least to some extent, benzylselenyl radicals had added to the isonitrile and that β-scission had taken place. No spectroscopic evidence of the selenoimidoyl radical **8Cf** was, however, obtained.

By analogy with thioimidoyls, selenoimidoyls with Se-alkyl (non-resonance-stabilized) substituents should be less susceptible to β-scission, and therefore the di-*i*-propyl diselenide **7b** was prepared and photolyzed with **4C**. No selenoimidoyl or *i*-propyl radicals were detected by EPR spectroscopy in this case in the temperature range 150−200 K. However, GC−MS analysis of the product mixture established again that *tert*-butyl isoselenocyanate **9** was a major product. We tentatively conclude from this that the selenoimidoyl radicals **8**, although not observable by EPR spectroscopy, are initially generated and undergo a fast β-scission to **9** (see, however, below).

Kinetics of Thioimidoyl β-Scission. The mechanism of the process taking place under EPR conditions may be represented by eqs 1−5:

$$\underset{\mathbf{4}}{R^1{-}NC} + {}^{\bullet}X{-}R^2 \xrightarrow{k_a} \underset{\mathbf{6}}{R^1NC^{\bullet}XR^2} \quad (1)$$

$$\mathbf{6} \xrightarrow{k_f} R^1NCX + R^{2\bullet} \quad (2)$$

$$R^{2\bullet} + R^{2\bullet} \xrightarrow{2k_t} \text{nonradical products} \quad (3)$$

$$R^{2\bullet} + \mathbf{6} \xrightarrow{k_x} \text{nonradical products} \quad (4)$$

$$\mathbf{6} + \mathbf{6} \xrightarrow{2k_t} \text{nonradical products} \quad (5)$$

(10) Danen, W. C.; West, T. *J. Am. Chem. Soc.* **1973**, *95*, 6872−6874.

(11) Recent theoretical work has suggested that the bent σ-structure is essentially independent of the electronic nature of the α-substituent: Guerra, M. *J. Phys. Chem.* **1996**, *100*, 19350.

(12) (a) Berndt, A. In *Landolt-Börnstein; Magnetic Properties of Free Radicals*, Fischer, H., Hellwege, K., Eds.; Springer: Berlin, 1977; Vol. 9b, p 452. (b) Berndt, A. In *Landolt-Börnstein; Magnetic Properties of Free Radicals*, Fischer, H., Hellwege, K., Eds.; Springer: Berlin, 1987; Vol. 17c, p 88.

TABLE 2. Rate and Arrhenius Parameters for Fragmentations of Thioimidoyl and Oxyimidoyl Radicals

	radical β-scission	k_f, s^{-1} (200 K)	log (A_f, s^{-1})	E_f (E_{13}),[a] kcal/mol	RSE,[b] kcal/mol
6Aa	*n*-$C_{12}H_{25}N{=}C^{\bullet}S$-*n*-Bu	7.0	14.0	12.0 (10.9)	3.9
6Ab	*n*-$C_{12}H_{25}N{=}C^{\bullet}S$-*i*-Pr	39	11.0	8.6 (10.6)	6.4
6Ad	*n*-$C_{12}H_{25}N{=}C^{\bullet}S$-*c*-$C_5H_9$	430	12.4	8.9 (9.5)	7.3
6Ac	*n*-$C_{12}H_{25}N{=}C^{\bullet}S$-*t*-Bu	1600	10.2	6.4 (8.7)	8.9
6Ba	*c*-$C_6H_{11}N{=}C^{\bullet}S$-*n*-Bu	12	13.2	11.1 (10.9)	3.9
6Bb	*c*-$C_6H_{11}N{=}C^{\bullet}S$-*i*-Pr	230	12.1	9.0 (9.8)	6.4
6Ca	*t*-Bu$N{=}C^{\bullet}S$-*n*-Bu	11	14.0	11.9 (10.7)	3.9
6Cb	*t*-Bu$N{=}C^{\bullet}S$-*i*-Pr	120	13.2	10.2 (10.0)	6.4
6Cd	*t*-Bu$N{=}C^{\bullet}S$-*c*-C_5H_9	680	12.8	9.2 (9.3)	7.3
6Cc	*t*-Bu$N{=}C^{\bullet}S$-*t*-Bu	3500	10.0	5.9 (8.4)	8.9
6Cg	*t*-Bu$N{=}C^{\bullet}SCH_2C{\equiv}CEt$	$\geq 4 \times 10^5$	[13]	($\leq$6.7)[c]	12.4
6Da	Ad$N{=}C^{\bullet}S$-*n*-Bu	12	13.0	10.9 (10.9)	3.9
6Db	Ad$N{=}C^{\bullet}S$-*i*-Pr	160	12.6	9.5 (9.9)	6.4
6Dc	Ad$N{=}C^{\bullet}S$-*t*-Bu	2400	12.6	8.5 (8.8)	8.9
	n-$C_{12}H_{25}N{=}C^{\bullet}O$-*t*-Bu	100	10.7	7.6	
	c-$C_6H_{11}N{=}C^{\bullet}O$-*t*-Bu	18	11.0	8.9	
	t-Bu$N{=}C^{\bullet}O$-*t*-Bu	50[d]	12.2[d]	9.6[d]	

[a] E_{13} are the experimental β-scission activation energies standardized under the assumption that log (A_f, s^{-1}) = 13. [b] Methane-based stabilization energies of the released C-centered radicals. [c] Estimated (see text). [d] Data from Roberts et al.[4]

By application of the steady-state approximation, it can easily be shown that

$$\frac{1}{[R^{2\bullet}]} = \frac{k_x}{k_f} + \frac{2k_t[R^{2\bullet}]}{k_f[\mathbf{6}]} \qquad (6)$$

Because the radicals involved are "small" molecules, the termination rate constants will be close to the diffusion rate and may all be considered the same[15] ($k_x = 2k_t$); hence eq 6 simplifies to the usual expression:

$$\frac{k_f}{2k_t} = [R^{2\bullet}] + \frac{[R^{2\bullet}]^2}{[\mathbf{6}]} \qquad (7)$$

For representative pairs of reactants, the corresponding thioimidoyl β-scission (fragmentation) rate constants (k_f) were therefore obtained from EPR spectroscopic measurements of the concentrations of the two radicals by the usual method with DPPH as standard.[16] The well-established $2k_t$ value of Schuh and Fischer,[17] corrected for the difference in viscosity between *n*-heptane and cyclopropane as described previously,[18] was introduced to enable absolute values of k_f to be derived. The Arrhenius plot of the data obtained for the *N*-*tert*-butyl-*S*-*i*-propyl-thioimidoyl radical **6Cb** derived from *tert*-butyl isonitrile and di-*i*-propyl disulfide (Figure 3) gives an example of the quality of the data obtained. All of the Arrhenius plots, with their linear regression equations, and examples of the EPR spectra are in the Supporting Information; the measured fragmentation rate constants are given in Table 2.

The data reported in Table 2 show that β-scission of the S−C bonds in thioimidoyl radicals is a fast process ($10^5 < k_f < 10^6$ s^{-1}) at 298 K. Thus, practically every kind of C-centered radical can be efficiently produced by this route at $T \geq 20$ °C. The rate of S−C bond scission in thioimidoyls is ≥16 times the rate of O−C bond scission in oxyimidoyls at 200 K. This is in accord with expectation because of the longer and weaker C−S bonds. Unfortunately, the β-scission rate constants for selenoimidoyl radicals could not be calculated by experimental data and an estimate will be reported in the theoretical section (see below). Blum and Roberts reported[4] the only previous kinetic datum for a thioimidoyl radical β-scission, i.e., k_f (243 K) = 3.1×10^5 s^{-1} for *t*-BuNC$^{\bullet}$S-*t*-Bu (**6Cc**). Extrapolation of our Arrhenius data (Table 2, E_{13}) for this radical gives k_f (243 K) = 2.8×10^5, in good agreement.

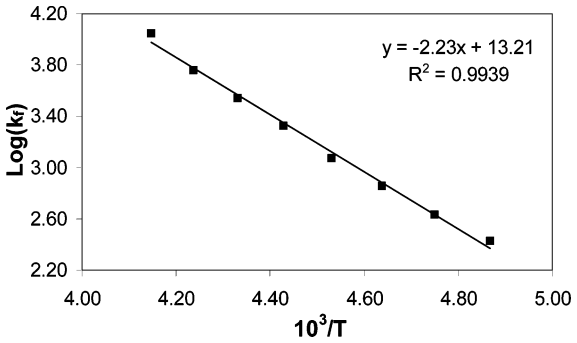

FIGURE 3. Arrhenius plot for β-scission of *N*-*t*-butyl-*S*-*i*-propyl-thioimidoyl radical **6Cb**.

Comparing the β-scission rate constants of the set of thioimidoyl radicals with *S*-*n*-Bu groups (or the set with *S*-*t*-Bu groups, Table 2) suggests that *N*-alkyl substituents have little influence on the rate. The rate constants are more variable for other *S*-groups but, bearing in mind that the error limits on the data are large, it is probable that the effect of *N*-substituents is minor. *S*-Alkyl substituents, on the other hand, have a dramatic effect, and going from *S*-*n*-alkyl to *S*-*tert*-butyl causes a rate increase of ca. 2 orders of magnitude at 200 K. The rate increase is even larger on going to a resonance-stabilized *S*-group such as allyl or benzyl (see above). These trends make it clear that two factors are important: (i) greater branching at the C-atom attached to sulfur dramatically increases the rate of fragmentation, and (ii) resonance

(13) Note, however, that Blum and Roberts[4] observed C−N β-scission of *t*-Bu$N{=}C^{\bullet}$OMe to afford the EPR spectrum of *t*-Bu$^{\bullet}$ radicals at higher temperatures.

(14) An experiment with *n*-propane as solvent showed no interpretable spectra in the range 110−150 K.

(15) Fischer, H.; Paul, H. *Acc. Chem. Res.* **1987**, *20*, 200.

(16) (a) Griller, D.; Ingold, K. U. *Acc. Chem. Res.* **1980**, *13*, 193. (b) Griller, D.; Ingold, K. U. *Acc. Chem. Res.* **1980**, *13*, 317.

(17) Schuh, H.; Fischer, H. *Helv. Chim. Acta* **1978**, *61*, 2130.

(18) Maillard, B.; Walton, J. C. *J. Chem. Soc., Perkin Trans. 2* **1985**, 443.

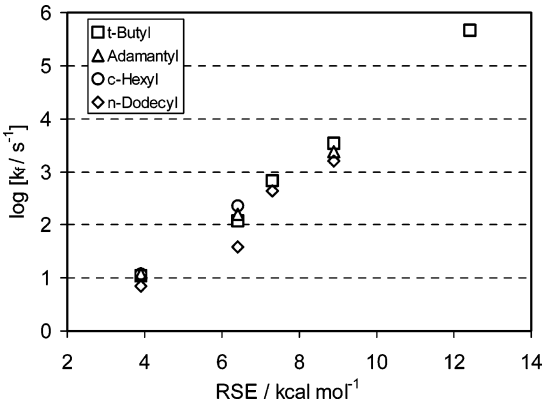

FIGURE 4. Plot of experimental log (k_f) values for thioimidoyl radicals vs methane-based radical stabilization energies (RSE) derived from thermochemical BDEs.

stabilization in the released radical also strongly increases the rate of fragmentation. Both these factors contribute to the thermodynamic stabilization energy of the released radical. In fact, a reasonably linear correlation is obtained from the methane-based stabilization energies of the C-centered radicals (RSE), derived from the difference in the recommended C−H bond dissociation energy (BDE) of methane and those of the corresponding hydrocarbons [BDE(R^2H)],[19,20] with the log (k_f) values (Figure 4). In deriving this correlation, a lower limit for the β-scission rate constant of the alk-2-ynyl thioimidoyl radical **6Cg** was estimated from the fact that only the pent-2-ynyl and not the corresponding thioimidoyl was observable in cyclopropane solution at 150 K. From the measured concentration of the released pent-2-ynyl radical, and assumption of the minimum thioimidoyl radical concentration consistent with the baseline S/N, the k_f shown in Table 2 was derived. The good linearity of this correlation ($r^2 = 0.967$) indicates that the stabilization of the released radical is a key factor in controlling the rate of fragmentation. Of course, changes in the strength of the bond being broken due to increased frontal strain with increasing branching of the substituent is an interrelated factor.

The literature provides very few examples of rate data for radical fragmentation processes involving C−S bond breaking. The exception is data for reactions of RS−CH_2-$CH^{\bullet}R'$ radicals undergoing β-scission with release of RS$^{\bullet}$ radicals and an alkene. Several such fragmentations have rate constants in the range 10^7−10^8 s^{-1} at 300 K and are therefore faster than thioimidoyl fragmentation.[21] Although both reactions involve β-scission of initially C-centered radicals via C−S bond breaking, the fragmentation of RS−$CH_2CH^{\bullet}R'$ radicals differs from that of thioimidoyls in that C=C bonds and sulfanyl radicals are formed compared with isothiocyanate moieties and alkyl radicals.

It is instead instructive to compare the behavior of imidoyls with that of alkoxycarbonyl radicals (O)$C^{\bullet}$O−R, which are isoelectronic with imidoyls but fragment by scission of O−C bonds with concomitant formation of C=O double bonds (elimination of carbon dioxide).[22] At room temperature, the fragmentations of *O-tert*-butyl oxyimidoyls (~1×10^5 s^{-1} at 298 K) are nearly as fast as those of the analogous *O-tert*-butyl carbonyl (1×10^5 s^{-1} at 293 K),[22b,c] whereas scissions of *S-tert*-butyl thioimidoyls are 3−20 times faster, in agreement with the weaker C−S bond. Interestingly, a comparison between various heteroatom-alkyl-substituted radicals shows that the fragmentation rate of alkoxycarbonyls is very sensitive to the released radical, passing from 2×10^2 s^{-1} for primary alkyls to 5×10^2 s^{-1} for secondary radicals and to as much as 1×10^5 s^{-1} for tertiary and (cyclopropyl)-methyl radicals (1:2.5:550 rate ratio at 293 K).[22c] By way of contrast, at room temperature, the fragmentations of the corresponding thioimidoyls are always faster and much less dependent on the extent of branching of the *S*-alkyl substituent, ranging from ~10^5 to ~10^6 s^{-1} at 298 K. Thus, despite the formation of a very stable fragmentation product (carbon dioxide), alkoxycarbonyls are quite reluctant to release primary or secondary radicals, which can be instead efficiently produced starting from thioimidoyls. Although the stabilization of the released radical remains a key factor in controlling the rate of fragmentation in thioimidoyls (see below), nevertheless its influence on the rate seems to be less important compared to alkoxycarbonyls; this is probably the result of early (alkoxycarbonyls)[22d] or late (thioimidoyls) transition states in which the X−C bond is broken to very different extents (see the section on theoretical calculation for further details).

The photoinitiated reaction of 1-dodecaneisonitrile (**4A**) with DTBP in cyclopropane showed spectra of a mixture of the cyclopropyl radical, derived from H-abstraction from the solvent by *t*-BuO$^{\bullet}$ radicals, and the *n*-$C_{12}H_{25}N$=$C^{\bullet}$O-*t*-Bu radical in the temperature range 150−195 K. At T > 230 K the *tert*-butyl radical started to appear. For the competition below 195 K (eqs 8 and 9)

$$^{t}\mathrm{BuO}^{\bullet} + \mathbf{4A} \xrightarrow{k_a} {}^{n}\mathrm{C_{12}H_{25}NC^{\bullet}O^{t}Bu} \qquad (8)$$

$$^{t}\mathrm{BuO}^{\bullet} + {}^{c}\mathrm{C_3H_6} \xrightarrow{k_H} {}^{t}\mathrm{BuOH} + {}^{c}\mathrm{C_3H_5}^{\bullet} \qquad (9)$$

it can easily be shown that

$$\frac{k_a}{k_H} = \frac{[{}^{n}\mathrm{C_{12}H_{25}NC^{\bullet}O^{t}Bu}][{}^{c}\mathrm{C_3H_6}]}{[{}^{c}\mathrm{C_3H_5}^{\bullet}][{}^{n}\mathrm{C_{12}H_{25}NC}]} \qquad (10)$$

From EPR measurements of the radical concentrations from two different *c*-C_3H_6 concentrations, a good, linear Arrhenius plot of k_a/k_H was obtained (see Supporting Information). Combining this with the known[23] Arrhenius parameters for k_H gave

$$k_a(\mathrm{M^{-1}\ s^{-1}}) = 10.3 - 7.0\ (\mathrm{kcal\ mol^{-1}})/\theta \qquad (11)$$

and hence at 290 K the rate constant for *t*-BuO$^{\bullet}$ radical addition to isonitrile **4A** is 1.2×10^5 M^{-1} s^{-1}. This is slightly smaller than the only other known rate constant of this type, i.e., k_a (290 K) = 2.6×10^5 M^{-1} s^{-1} for addition of *t*-BuO$^{\bullet}$ to *t*-BuNC reported by Roberts and

(19) (a) Seetula, J. A.; Russell, J. J.; Gutman, D. *J. Am. Chem. Soc.* **1990**, *112*, 1347. (b) Seetula, J.; Gutman, D. *J. Phys. Chem.* **1992**, *96*, 5401. (c) Berkowitz, J.; Ellison, G. B.; Gutman, D. *J. Phys. Chem.* **1994**, *98*, 2744.

(20) Cohen, N. In *General Aspects of the Chemistry of Radicals*; Alfassi, Z. B., Ed.; Wiley: Chichester, U.K., 1999; Chapt. 10, p 317.

(21) Chatgilialoglu, C.; Altieri, A.; Fischer, H. *J. Am. Chem. Soc.* **2002**, *124*, 12816.

co-workers.[4,24] These rate constants show that *t*-butoxyl radical addition to N=C of isonitriles is somewhat slower than addition to C=C of alkenes [k_a (300 K) ~ 10^6] but is still a fast process. This is in good accord with the known efficiency of this and related radical additions to isonitriles in a variety of synthetic procedures.

As far as the selenoimidoyls are concerned, the fragmentation rate constants could be neither calculated nor estimated from the spectra of similar thioimidoyls. Indeed, the photolyses of disulfides or diselenides in the presence of an isonitrile are probably not fully comparable, due to the presence of significant side reactions with seleno compounds.

Photolysis of dialkyl diselenides is known to afford products deriving also from scission of the C−Se bond in addition to those derived from Se−Se bond fragmentation.[25] The presence of major amounts of dibenzyl in the reaction of diselenide **7f** with **4C**, compared to the yield of isoselenocyanate **9**, suggests that great amounts of benzyl radical could be formed by homolysis of the $PhCH_2$−Se bond rather than fragmentation of selenoimidoyl **8Cf** (which forms nonetheless, but probably to a minor extent). With diselenide **7b** the reaction afforded greater amounts of isoselenocyanate **9**, probably as a result of the major formation of selenoimidoyl **8Cb**, but neither selenoimidoyl nor *i*-propyl radicals were detected. The absence of any signal ascribable to the selenoimidoyl could be due either to the effect of the selenium atom on the relaxation time of the radical, with the effect of broadening the lines beyond detection, or to a very fast fragmentation process that might prevent buildup of radical concentration. However, the lack of any signal of the *i*-propyl radical suggested the presence in the reaction medium of some very fast reactions that would be able to scavenge those species as soon as they formed. A possible scavenging route could be an intermolecular homolytic substitution of the *i*-propyl radicals onto the Se−Se bond of the starting diselenide, which is a known, fast reaction that could also take place with disulfides, although at a significantly lower rate.[26,27]

To verify whether this process could appreciably affect the concentration of the alkyl radicals in the reactions of both disulfides and diselenides, the kinetic law obtained above (eq 7) was modified to take the intermolecular S_H2 process (eq 12) into account; eq 13 was thus obtained, where k_{HS} is the rate constant for intermolecular substitution of $R^{2\bullet}$ radicals on the dichalcogenide:

$$R^{2\bullet} + R^2XXR^2 \xrightarrow{k_{HS}} R^2XR^2 + R^2X^{\bullet} \qquad (12)$$

$$\frac{k_f}{2k_t} = [R^{2\bullet}] + \frac{[R^{2\bullet}]^2}{[\mathbf{6}]} + \frac{k_{HS}[R^{2\bullet}][R^2XXR^2]}{2k_t[\mathbf{6}]} \qquad (13)$$

From the reported data of 6×10^4 M^{-1} s^{-1} and 3×10^7 M^{-1} s^{-1} (at 25 °C) for the addition of primary alkyl radicals to dimethyl disulfide and diphenyl diselenide, respectively,[26] we tentatively estimated the variations in the activation energies of fragmentations of thio- and selenoimidoyls by assuming an average value of ca. 0.25 M for the concentration of the dichalcogenide. The Arrhenius plots (see Figure 3) were recalculated by means of eq 13, giving, for thioimidoyls, very minor changes in the activation energies (≤2%): this confirms that the S_H2 process does not influence the kinetic outcome to significant extents and use of eq 7 instead of eq 13 is a very good approximation.[4] On the contrary, the greater value of k_{HS} for selenoimidoyls, in conjunction with eq 13, gave activation-energy differences that can be as large as 1−1.5 kcal mol^{-1} with respect to eq 7. This supports the contention that the reactions of thio- and selenoimidoyl radicals are not totally comparable and the former cannot be used to acceptably estimate the β-scission rate constants for the latter. Indeed, small errors in the estimation could result in activation-energy differences that do not allow us to establish whether selenoimidoyls fragment faster than thioimidoyls or vice versa (see computational section).

Ring Closures of *S*-Alk-3-enyl Thioimidoyl Radicals. The k_f values for all the $R^1N{=}C^{\bullet}S$-*n*-Bu radicals were close to 10^5 s^{-1} at 300 K. That is marginally less than the rate constants of many ring closure reactions. For example, the archetype hex-5-enyl radical cyclizes with a rate constant of 2.3×10^5 s^{-1} at 300 K.[28] This indicated that thioimidoyl radicals with primary *S*-alkenyl (or *S*-alkynyl) substituents might be able to cyclize before fragmentation under certain circumstances. Ring closure onto the *S*-alkenyl group would produce dihydrothiophen-2-ylidene amines (e.g., **14**) that could easily be hydrolyzed, thus affording γ-butyrothiolactones by a novel radical route.

To test the feasibility of this idea, dibut-3-enyl disulfide **5i** was prepared and photolyzed with several isonitriles. When dodecane-1-isonitrile **4A** was used, broad unidentified spectra were obtained. However, when adamantane-1-isonitrile **4D** was employed, a strong EPR spectrum of the expected thioimidoyl radical **6Di** was observed in the temperature range 170−220 K (Table 1). At higher temperatures, two additional radicals appeared (Figure 5). One of these (marked B) was the but-3-enyl radical **10** with hfs identical to those in the literature.[29] The other radical (marked C) had $g = 2.0027$, $a(2H) = 21.8$, $a(1H) = 30.9$, and $a(1H) = 0.9$ G and can be positively identified

(22) For some representative papers on alkoxycarbonyl radicals, see (with references therein) (a) Forbes, J. E.; Zard, S. Z. *J. Am. Chem. Soc.* **1990**, *112*, 2034. (b) Beckwith, A. L. J.; Bowry, V. W. *J. Am. Chem. Soc.* **1994**, *116*, 2710. (c) Simakov, P. A.; Martinez, F. N.; Horner, J. H.; Newcomb, M. *J. Org. Chem.* **1998**, *63*, 1226. (d) Morihovitis, T.; Schiesser, C. H.; Skidmore, M. A. *J. Chem. Soc., Perkin Trans. 2* **1999**, 2041.

(23) Walton, J. C.; McCarroll, A. J.; Chen, Q.; Carboni, B.; Nziengui, R. *J. Am. Chem. Soc.* **2000**, *122*, 5455.

(24) The k_a value from ref 4 was recalculated with more recent Arrhenius data for the reference reaction, i.e., the H-abstraction from cyclopentane; see Baban, J. A.; Goddard, J. P.; Roberts, B. P. *J. Chem. Soc., Perkin Trans. 2* **1986**, 269.

(25) See, for example, Franzi, R.; Geoffroy, M. *J. Organomet. Chem.* **1981**, *218*, 321.

(26) Curran, D. P.; Martin-Esker, A. A.; Ko, S.-B.; Newcomb, M. *J. Org. Chem.* **1993**, *58*, 4691.

(27) The feasibility of the S_H2 process of alkyl radicals onto the dichalcogenide was also supported by the presence of dibutenyl sulfide among the reaction products of disulfide **5i** with isonitrile **4C** (see the section on cyclization). Although this product could also form by coupling of butenyls with sulfanyl radicals, it is likely that the major formation pathway is actually intermolecular attack of the butenyl radicals onto the starting disulfide.

(28) Chatgilialoglu, C.; Ingold, K. U.; Scaiano, J. C. *J. Am. Chem. Soc.* **1981**, *103*, 7739.

(29) Kochi, J. K.; Krusic, P. J.; Eaton, D. R. *J. Am. Chem. Soc.* **1969**, *91*, 1877.

as the 2-substituted dihydrothiophenylmethyl radical **11D**.

Very similar spectra containing signals from the three analogous radicals were obtained when **5i** was photolyzed together with *tert*-butyl isonitrile **4C**.[8] These observations confirmed that ring closure onto the *S*-butenyl substituent of a thioimidoyl radical could take place and that the preferred mode was *5-exo*. Above ca. 280 K all the thioimidoyl radicals were converted to but-3-enyl and dihydrothiophenylmethyl radicals with the former predominating.

Cyclopropane is a poor hydrogen-atom donor and therefore, under EPR conditions, the main products were expected to be the isothiocyanate (R^1NCS) together with compounds from combination and disproportionation of the three radicals. The main products identified by GC−MS analyses of several photoinitiated reactions of **5i** with **4C** (R^1 = *t*-Bu) are shown in Scheme 4 (see the Experimental Section for minor products). Product analysis of the reaction of **5i** with **4D** showed similar results but the conversion was lower, so individual components were more difficult to characterize.

Product analysis confirmed that disproportionation (e.g., **14**, **15**), combination (**18**), and cross-combination (e.g., **13**) of the intermediate radicals **6**, **10**, and **11** were the dominant processes. Butane, butene, and octa-1,7-diene from the but-3-enyl radicals were not observed because of their volatility. A small amount (0.4%) of a second product having $M^+ = 171$ ($C_9H_{17}NS$) was also formed. This can probably be identified as the *N-tert*-butyl-(tetrahydropyran-2-ylidene)amine **16**. Comparing the yield of this disproportionation product with that of **14** suggested the *5-exo*/*6-endo* cyclization ratio was ca. 35:1 at 0 °C. Product analysis agreed with the reaction mechanism shown in Scheme 4, except that minor amounts of products derived from reactions of the butenylsulfanyl radical, e.g., **19**, were also implicated (<10% total). If one neglects the minor amount of termination involving butenylsulfanyl and assumes diffusion control, it can easily be shown that eqs 14 and 15 hold:

$$\frac{k_c}{2k_t} = [\mathbf{11}] + \frac{[\mathbf{11}]^2}{[\mathbf{6}]} + \frac{[\mathbf{10}][\mathbf{11}]}{[\mathbf{6}]} \qquad (14)$$

$$\frac{k_f}{2k_t} = [\mathbf{10}] + \frac{[\mathbf{10}]^2}{[\mathbf{6}]} + \frac{[\mathbf{10}][\mathbf{11}]}{[\mathbf{6}]} \qquad (15)$$

The concentrations of radicals **6**, **10,** and **11** were determined, by the EPR spectroscopic method described above, for initial isonitriles **4C** and **4D**. Substitution into eqs 14 and 15 led to the rate parameters listed in Table 3.

Comparison of the β-scission rate data [k_f(200 K) etc.] of the *S*-but-3-enyl thioimidoyl radicals with the analogous data for $R^1N{=}C^{\bullet}S$-*n*-alkyl radicals in Table 2 shows they are strikingly similar, and this lends confidence to the reliability of the data, as does the fact that the R^1 = Ad and R^1 = *t*-Bu data are also nearly equal. At 200 K the cyclization rates are higher than the β-scission rates, but the reverse is true at 300 K. It follows that for these systems β-scission will be the major reaction channel at temperatures usual for synthetic procedures.

The measured cyclization rate parameters were very similar for the two *S*-but-3-enyl thioimidoyl radicals

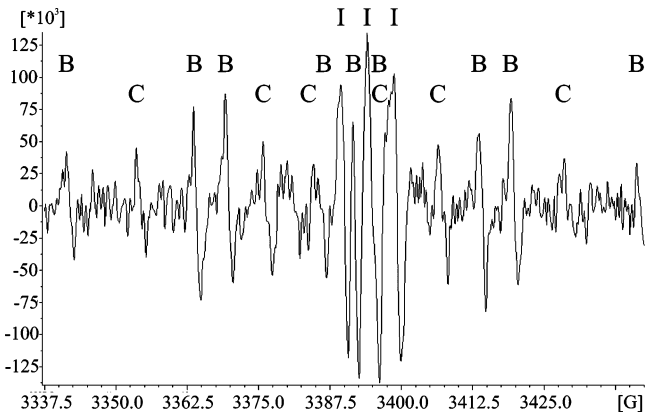

FIGURE 5. EPR spectrum resulting from photolysis of isonitrile **1D** and disulfide **5i** at 250 K.

SCHEME 4

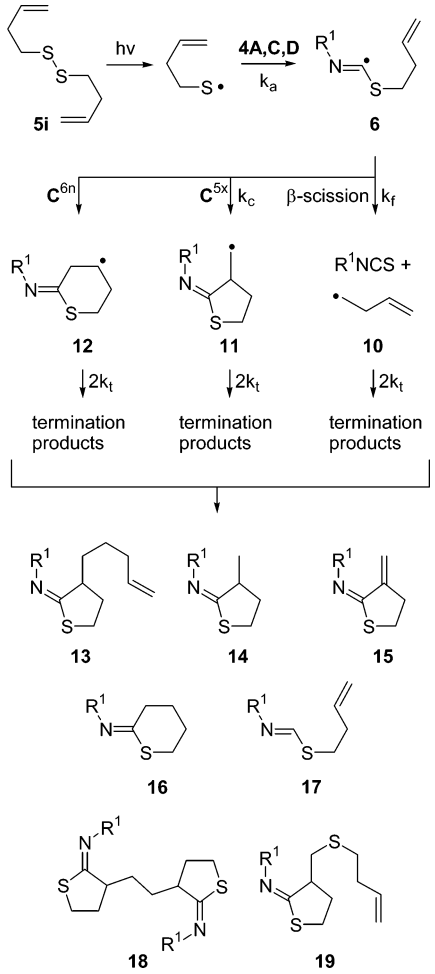

(Table 3); thus, as expected, the R^1-N substituent is too far from the radical center to have much effect on the rate. These kinetic data are the first available for ring closure of any type of imidoyl radical. The regioselectivity is strongly in favor of *5-exo* cyclization, as is usual for C-centered species.

Thioimidoyl radicals are isoelectronic with acyl radicals such as 1-hexanoyl and the latter is also a σ-type species. Acyl radicals show a preference for *6-endo* ring closure under certain conditions,[30] but this is due to rearrangement of the initial 2-oxocyclopentylmethyl radical via a

TABLE 3. Rate and Arrhenius Parameters for Unimolecular Reactions of *S*-But-3-enyl Thioimidoyl Radicals

	cyclization of	k_c at 300 K [200 K], s^{-1}	log (A_c, s^{-1})	E_c, kcal/mol
6Ci	*t*-BuN=C•S$(CH_2)_2$CH=CH_2	2.4×10^4 [45]	10.2	8.0
6Di	AdN=C•S$(CH_2)_2$CH=CH_2	3.8×10^4 [28]	10.5	8.0
	β-scission of	k_f at 300 K [200 K], s^{-1}	log (A_f, s^{-1})	E_f, kcal/mol
6Ci	*t*-BuN=C•S$(CH_2)_2$CH=CH_2	2.0×10^5 [8]	13.7	11.7
6Di	AdN=C•S$(CH_2)_2$CH=CH_2	1.6×10^5 [13]	13.7	11.6

TABLE 4. Calculated Δ*H* Values and Activation Energies for *β*-Fragmentations of Some Thioimidoyl Radicals[a]

		computed values[b]				
		β-scission N-R^1 side		β-scission S-R^2 side		
	radical (R^1N=C•S-R^2)	Δ*H*	E_a	Δ*H*	E_a	exp data E_a[c] (analogous radical)
6Fk	EtN=C•SEt	9.9	21.2	−0.13	9.4	12.0 (**6Aa**)
6Gb	*i*-PrN=C•S-*i*-Pr	7.6	19.3	−2.6	7.0	9.0 (**6Bb**)
6Cc	*t*-BuN=C•S-*t*-Bu	4.5	15.4	−6.4	4.4	5.9 (**6Cc**)

[a] All energy values (Δ*H* and E_a) are in kilocalories per mole. [b] Computed by the UB3LYP method with a 6-31+G(2d,p) basis set. [c] Experimental activation energy for β-fragmentation at the S-R^2 side of analogous radicals (see Table 2).

bicyclo[4.1.0]hexanoxyl radical. A similar rearrangement of **6** could be envisaged via **20**, but thermodynamic control, which is a condition for this process to compete, is most unlikely to prevail at the low temperatures of the EPR experiments and no evidence of ring expansion was obtained.

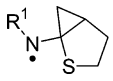

20

Comparison with model species such as hex-5-enyl (see above) shows that ring closure of **6Ci** is about an order of magnitude slower at 300 K. This is probably not a consequence of the N= substitution at the radical center, because analogous O= substitution did not depress the rate of cyclization of hex-5-enoyl [k_c (300 K) = 2.2×10^5 s^{-1}][31] compared to hex-5-enyl. Cyclization of **6Ci** is also slower than that of the isoelectronic (but-3-enyloxy)-carbonyl radical[22c] ($k_c = 1.7 \times 10^5$ s^{-1} vs 4×10^6 s^{-1} at 80 °C).

Replacement of the α-methylene group of the hex-5-enyl radical with a $SiMe_2$ group led to a significant reduction in k_c (to 7.5×10^3 s^{-1} at 298 K).[32] This was attributed to bond length effects, which made it difficult for the radical center to approach the CCH end of the double bond. Analogous bond length effects explain the slower *5-exo* cyclization rates of thioimidoyl radicals **6Ci** and **6Di** and suggest that slower ring closure rates may be general for radicals with second- (and subsequent) row groups α- to C-centered hex-5-enyl type radicals. Ring closure reactions of the archetype **6Xi** will not be useful for preparing dihydrothiophen-2-ylidene amines because *β*-scission is too rapid. However, our results serve the useful purpose of showing that only a small increase in the rate of cyclization, for example, by inclusion of an electron-withdrawing substituent at the terminus of the double bond (Ph, CO_2R), should tip the balance in favor of ring closure.

Computational Study of Imidoyl Radical *β*-Scission and Cyclization. To get a better insight into the structure and reactivity of imidoyl radicals, some theoretical calculations were carried out on both the fragmentation and the cyclization reactions by the DFT approach, UB3LYP variant.[33,34] Attention was first focused on the *β*-scission modes of the thioimidoyl series. Calculations were carried out on thioimidoyl radicals bearing primary, secondary, and tertiary alkyl groups on both nitrogen and sulfur (Table 4). For all species the enthalpy variations and the activation barriers were calculated for both *β*-fragmentation modes. Scission at the nitrogen side was found to be always endothermic and was characterized by quite high computed activation energies (15.4−21.2 kcal/mol); on the contrary, fragmentations at the sulfur side were always computed to be

(30) (a) Chatgilialoglu, C.; Crich, D.; Komatsu, M.; Ryu, I. *Chem. Rev.* **1999**, *99*, 1991. (b) Chatgilialoglu, C.; Ferreri, C.; Lucarini, M.; Venturini, A.; Zavitsas, A. A. *Chem. Eur. J.* **1997**, *3*, 376.

(31) Brown, C. F.; Neville, A. G.; Rayner, D. M.; Ingold, K. U.; Lusztyk, J. *Aust. J. Chem.* **1995**, *48*, 363.

(32) (a) Wilt, J.; Lusztyk, J.; Peeran, M.; Ingold, K. U. *J. Am. Chem. Soc.* **1988**, *110*, 281. (b) Wilt, J. *Tetrahedron* **1985**, *41*, 3979.

(33) Calculations were carried out with the Gaussian 98W package.[34] Density functional theory (DFT), UB3LYP variant, was employed. The equilibrium geometries were fully optimized with respect to all geometric variables with the 6-31+G(2d,p) (radicals **6Fk**, **6Gb**, and **6Cc**) and 6-311+G(d,p) (all other species) basis sets. For the calculation of thermodynamic properties, total energies were adjusted for zero-point vibrational energies and for thermal corrections to 298 K. Computed $\langle S^2 \rangle$ values were in the range 0.7530−0.7650 before annihilation and 0.7500 after annihilation of higher multiplicity spin states. The transition states for *β*-fragmentations (or cyclization) were optimized by performing a progressive elongation of the bond involved in the scission (or ring closure) and optimizing each single step (relaxed scan) with a small basis set (UB3LYP/6-31G). Eventually, the energy maximum was optimized with the usual basis set [6-31+G(2d,p)]. All the transition states were characterized by a unique imaginary frequency corresponding to the desired bond scission (see Supporting Information). Isotropic EPR hfs were derived from the computed Fermi contact integrals and were taken directly from the Gaussian output file.

(34) Frisch, M. J.; Trucks, G. W.; Schlegel, H. B.; Scuseria, G. E.; Robb, M. A.; Cheeseman, J. R.; Zakrzewski, V. G.; Montgomery, J. A., Jr.; Stratmann, R. E.; Burant, J. C.; Dapprich, S.; Millam, J. M.; Daniels, A. D.; Kudin, K. N.; Strain, M. C.; Farkas, O.; Tomasi, J.; Barone, V.; Cossi, M.; Cammi, R.; Mennucci, B.; Pomelli, C.; Adamo, C.; Clifford S.; Ochterski, J.; Petersson, G. A.; Ayala, P. Y.; Cui, Q.; Morokuma, K.; Salvador, P.; Dannenberg, J. J.; Malick, D. K.; Rabuck, A. D.; Raghavachari, K.; Foresman, J. B.; Cioslowski, J.; Ortiz, J. V.; Baboul, A. G.; Stefanov, B. B.; Liu, G.; Liashenko, A.; Piskorz, P.; Komaromi, I.; Gomperts, R.; Martin, R. L.; Fox, D. J.; Keith, T.; Al-Laham, M. A.; Peng, C. Y.; Nanayakkara, A.; Challacombe, M.; Gill, P. M. W.; Johnson, B.; Chen, W.; Wong, M. W.; Andres, J. L.; Gonzalez, C.; Head-Gordon, M.; Replogle, E. S.; Pople, J. A. *Gaussian 98*, revision A.11 2/3; Gaussian, Inc.: Pittsburgh, PA, 2002.

TABLE 5. Theoretical and Experimental Hyperfine Splitting Values for Some Thioimidoyl Radicals[a]

	computed spectra[b]				experimental spectra[b]		
	radical	a(N)	$a(H_\beta)$		radical	a(N)	$a(H_\beta)$
6Fk	EtN=C•SEt	3.59	1.74 (2H)	**6Aa**	n-$C_{12}H_{25}$N=C•S-n-Bu	4.12	1.98 (2H)
6Gb	i-PrN=C•S-i-Pr	4.37	6.51 (1H)	**6Bb**	c-C_6H_{11}N=C•S-i-Pr	4.64	2.20 (1H)
6Cc	t-BuN=C•S-t-Bu	5.26		**6Cc**	t-BuN=C•S-t-Bu	5.10	

[a] Computed by the UB3LYP method with a 6-31+G(2d,p) basis set. [b] All hyperfine splitting values are in gauss.

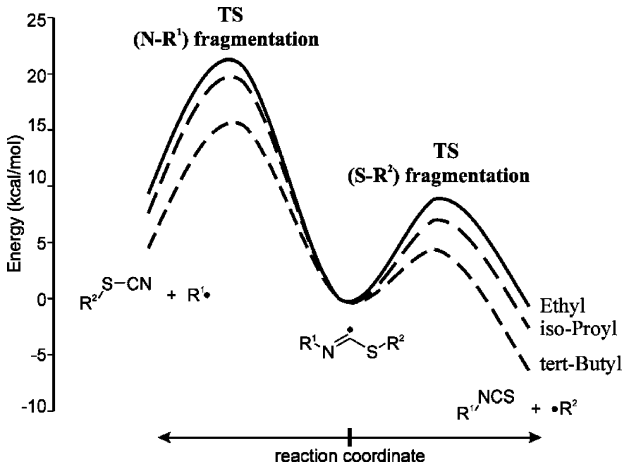

FIGURE 6. Theoretical fragmentation pathways for thioimidoyl radicals; for better comparison, all the energies were shifted so as to make the energies of the starting thioimidoyls equal to zero.

exothermic and had lower activation barriers (4.4−9.4 kcal/mol). Both modes became more and more favored, from both a thermodynamic and a kinetic point of view, by passing from primary to secondary and eventually to tertiary alkyl substituents. Figure 6 clearly shows that S−R^2 fragmentation was predicted to be always favored compared to the N−C scission, even when a primary radical (E_a = 9.4 kcal/mol) was released in competition with a tertiary one (E_a = 15.4 kcal/mol).

Table 4 also indicates that the calculated energies are slightly underestimated, in comparison with experimental data for identical (**6Cc**) or analogous (**6Bb**) thioimidoyls, as expected for this theoretical method.[35] On passing from primary to secondary and from secondary to tertiary alkyl groups, the percentage barrier variations (34% and 58%, respectively) are strictly comparable to the observed ones (34% and 52%, respectively).

Table 5 reports a comparison between calculated and experimental hfs values for the same radical species discussed in Table 4, and Figure 7 shows the optimized structures of thioimidoyls **6Fk**, **6Gb**, and **6Cc** as obtained by DFT calculations. As far as the a(N) data are concerned, very good agreement between calculated and experimental values was observed for all radicals (outstandingly for radical **6Cc**). Since the hfs are extremely sensitive to the geometry of the radical, theoretical results clearly support the EPR data in stating that thioimidoyls are σ-radicals with a bent structure and a trans configuration about the C=N double bond (Figure 7).

Again, for all radicals, the calculations predict negligible spin densities at the β-protons on the sulfur side,

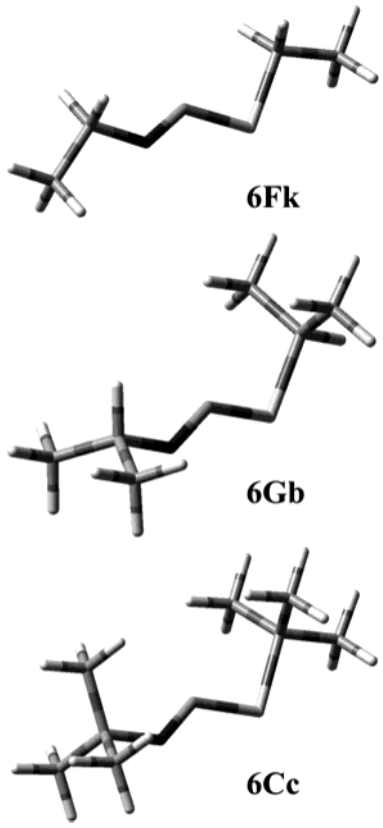

FIGURE 7. Optimized structures [UB3LYP, 6-31+G(2d,p) basis set] of thioimidoyls **6Fk**, **6Gb**, and **6Cc**.

in agreement with the recorded spectra. Good accord was also observed between predicted and experimental $a(H_\beta)$ values at the nitrogen side for radicals **6Fk** and **6Aa**, whereas calculations failed in estimating the $a(H_\beta)$ hfs for radicals bearing a secondary N-alkyl group (**6Gb**). In the latter case, this is probably due not to modifications in the radical core but rather to problems in optimizing the conformation of the N-alkyl chain.[36] Indeed, from the conformational analysis of radical **6Gb**, we could identify two degenerate relative minima in which a methyl group, instead of the hydrogen atom, is eclipsed with the orbital containing the unpaired electron; for these species a value of −0.98 was predicted for the $a(H_\beta)$ hfs. Taking into account the Boltzmann distribution and the energy gap between the two states, we could obtain a noteworthy decrease in the average $a(H_\beta)$ value, which was nevertheless still significantly different from the experimental one. Therefore, DFT calculations probably failed in estimating both the real conformational minimum and the energy gap between the possible conformers. It is

(35) Foresman, J. B.; Frisch, Æ. *Exploring chemistry with electronic structure methods*, 2nd ed.; Gaussian Inc.: Pittsburgh, PA, 1996.

(36) Analogous differences were found by replacing the c-hexyl group with other secondary chains.

SCHEME 5

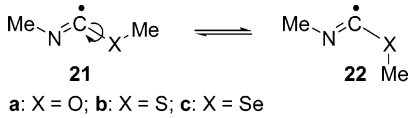

TABLE 6. Δ*H* Values and Activation Barriers for Isomerization of Radicals 21 and 22[a,b]

radicals	Δ*H*	E_a
21a → **22a** (X = O)	−0.86	5.1
21b → **22b** (X = S)	0.44	6.2
21c → **22c** (X = Se)	0.96	5.4

[a] Computed by the UB3LYP method with a 6-311+G(d,p) basis set. [b] All values are in kilocalories per mole.

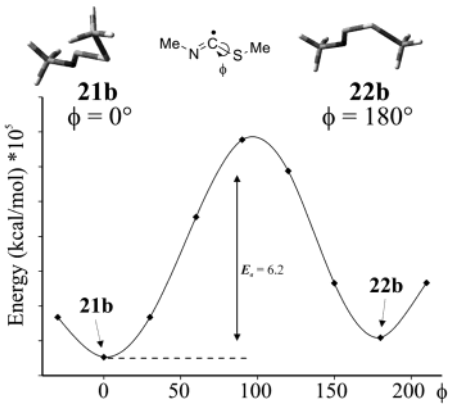

FIGURE 8. Energy profile for rotation of the C−S bond in thioimidoyls **21b** and **22b**. ϕ is the dihedral angle formed by the radical orbital and the C−S and S−Me bonds.

worth noting that MM calculations on conformer distribution for radical **6Gb** predicted a global minimum with the hydrogen atom not eclipsed with the radical center. We conclude that thioimidoyl **6Gb** probably stays longer than predicted by DFT methods in a staggered rather than an eclipsed conformation (with respect to the radical center), thus giving rise to the low $a(H_\beta)$ hfs observed in its EPR spectrum.

To probe the mechanism of the β-fragmentations, a more detailed theoretical study was carried out on this pathway for imidoyl radicals **21** with the 6-311+G(d,p) basis set (Scheme 5).

For all imidoyl radicals, rotation around the single C•−X bond resulted in two conformational minima corresponding to the *s-trans* (**21**) and *s-cis* (**22**) rotamers; for the oxyimidoyl (X = O), the absolute minimum is the *s-cis* structure **22a**, whereas for thio- (X = S) and selenoimidoyl (X = Se), the global minima correspond to the *s-trans* structures **21b**,**c**. Thermodynamic and kinetic data for rotation of the C•−X bond (i.e., isomerization of **21** into **22**) are reported in Table 6 and the energy profile for the isomerization is shown in Figure 8 for thioimidoyls **21b** and **22b**. It is worth noting that rotamers **21** have the W structure already postulated for analogous oxyimidoyls.[4b]

The activation energies for both fragmentation modes (*N*- and *X*-side) were calculated by starting from both radicals **21** and **22**. Independently of *X*, the transition states arising from structures **22** (TS N and TS X) were lower in energy with respect to those derived from

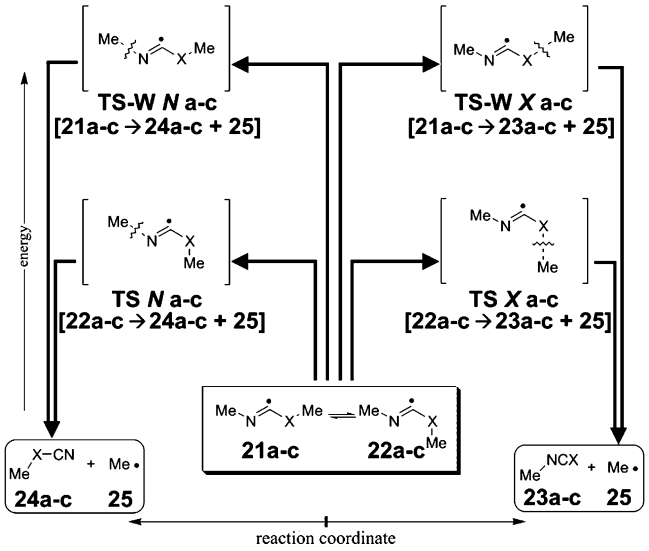

FIGURE 9. Fragmentation pathways for thioimidoyls **21a**−**c**/**22a**−**c**.

TABLE 7. Activation Energies for β-Fragmentations of Imidoyls 21a−c/22a−c[a,b]

	β-fragmentation *N*-side		β-fragmentation *X*-side	
radical	TS-W N (from **21**)	TS N (from **22**)	TS-W X (from **21**)	TS X (from **22**)
a (X = O)	29.4	27.5	24.1	10.5
b (X = S)	23.5	22.5	12.0	10.3
c (X = Se)	23.8	21.9	12.6	11.7

[a] Computed by the UB3LYP method with a 6-311+G(d,p) basis set. [b] All values are in kilocalories per mole.

intermediates **21** (TS-W N and TS-W X).[37] Figure 9 and Table 7 show all the evolution paths of radicals **21**/**22** and the related activation barriers.

For X = O, the oxyimidoyl radical stays in the preferred structure (**22a**) already capable of fragmenting at the O−Me side through the favored transition state (**TS X a**); the β-scission occurs with a Δ*H* of −16.9 kcal/mol and an activation barrier of 10.5 kcal/mol. Instead, for X = S and X = Se, taking into account that the imidoyl radicals prefer conformation **21** but the rotation barriers around the C•−X bond are always lower than those for β-fragmentations (Table 6), calculations suggest that the real evolution pathway should involve a two-step mechanism requiring prior conversion of **21b**,**c** into **22b**,**c**, followed by scission of the X−Me bond through the favored non-W transition state (**TS X b**,**c**). Loss of the alkyl group at the *X*-side seems therefore to resemble the anti elimination process typical of many ionic reactions. The fragmentations occur with Δ*H* values of 0.59 and 4.4 kcal/mol and E_a values of 10.3 and 11.7 kcal/mol for sulfur and selenium, respectively, so that fragmentations of thioimidoyls appear to be noticeably favored compared to those of analogous selenoimidoyls. As discussed above, β-fragmentations at the *N*-side never compete with β-scission at the *X*-side. The whole fragmentation mechanism is shown in Figure 10 for thioimidoyl **21b**.

It is worth pointing out that Table 7 shows that the computed activation barrier for fragmentation of sele-

(37) The activation energies reported in Table 4 are properly related to the favored non-W (**TS-X**-like) transition states.

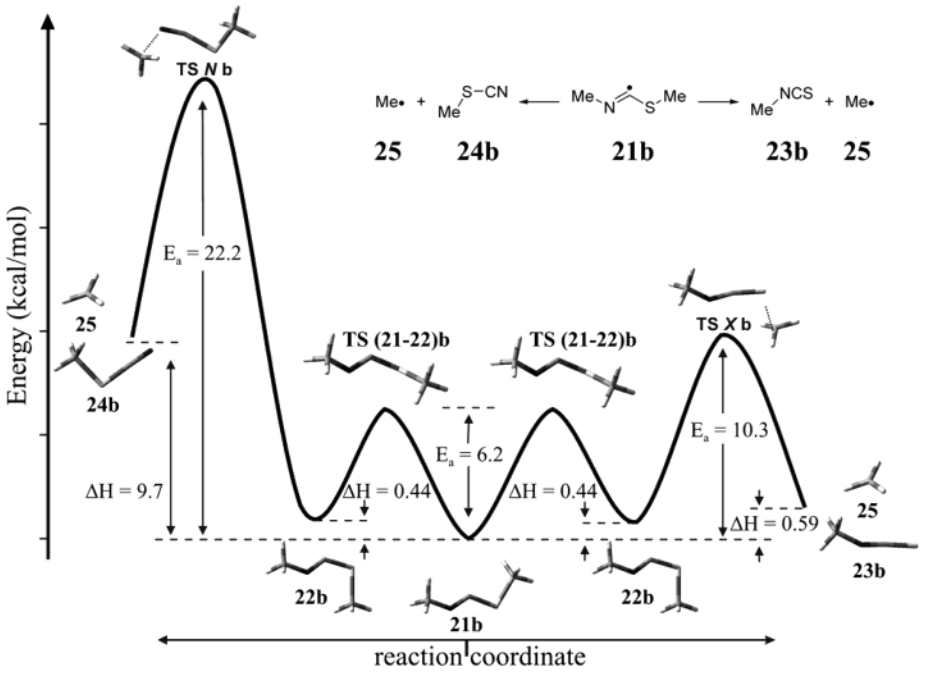

FIGURE 10. Whole fragmentation mechanism for thioimidoyl **21b** [UB3LYP method, 6-311+G(d,p) basis set, all values are in kilocalories per mole].

noimidoyl **21c**/**22c** is significantly higher than those of the analogous oxy- and thioimidoyl radicals **21a**,**b**/**22a**,**b**, probably because scission of the weak Se−C bond is associated with the formation of a much weaker isoselenocyanate moiety. Calculations therefore suggest that selenoimidoyls should be less prone to fragmentation compared to the analogous thioimidoyls; scission of the latter species seems moreover to be slightly favored even with respect to oxyimidoyls, in agreement with the experimental data (see Table 2).

Spin density maps and hfs were calculated for radicals **21a**−**c** and **22a**−**c** (see Supporting Information). Calculations predict very low *a*(N) values for X = O (−0.32 and −0.81 G for **21a** and **22a**, respectively), in agreement with the experimental data (Table 1). For X = S (3.68−3.39 G) and X = Se (3.65−3.48 G), the *a*(N) values are very close to each other, but selenium seems to be marginally more able to delocalize spin density compared to sulfur. Good agreement was again observed between calculated and experimental nitrogen hfs of thioimidoyls (3.68 G for **21b** vs 4.12 G for **6Aa**), whereas, unfortunately, no comparison with experimental data is possible for selenoimidoyls, since no selenoimidoyl radical has hitherto been detected.

As can be seen from Figure 11, the overall spin distribution in radicals **22a**−**c** is very different from that calculated for radicals **21a**−**c**. In particular, rotamers **22a**−**c** are characterized by a significant spin density on the *X*-methyl group, whereas isomers **21a**−**c** do not seem to distribute the spin on that moiety. This means that radicals **22a**−**c** show something akin to an embryonic formation of the methyl radical and are therefore more similar to the corresponding transition states (**TS X a**−**c**) than are radicals **21a**−**c** (**TS-W X a**−**c**): this could account for the lower activation energies calculated for all of the non-W **TS X** transition states. Figure 12 shows

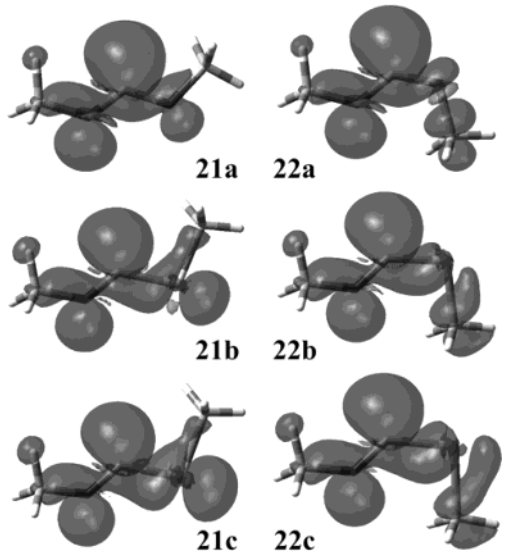

FIGURE 11. Spin density maps for radicals **21a**−**c** and **22a**−**c** [UB3LYP method, 6-311+G(d,p) basis set].

a comparison between the two rotamers and the corresponding transition states for thioimidoyls **21b**/**22b**.

We also simulated the ring closure of *S*-butenyl-substituted thioimidoyls by means of radical **6Ci** [UB3-LYP, 6-31+G(2d,p) basis set; see Supporting Information for computed EPR hfs of radicals **6Ci** and **11C**]. The cyclization of **6Ci** was slightly exothermic ($\Delta H = -3.1$ kcal/mol), with an activation barrier of 9.5 kcal/mol. In terms of activation energy, there is therefore good agreement with the experimental values (8.0 kcal/mol for both radicals **6Ci** and **6Di**). Nevertheless, the underestimation of the activation barrier for the associated fragmentation [≈9−10 kcal/mol (see Table 4, radical **6Fk**, and Table 7, radical **21b**) compared with the experimental values of

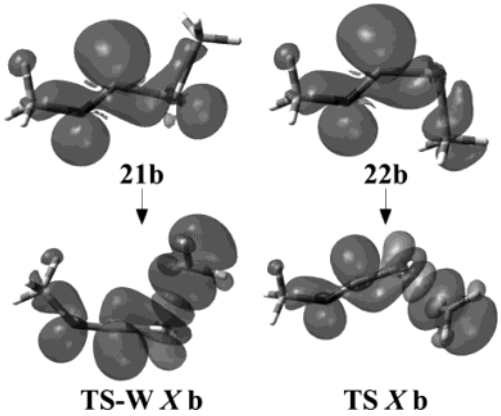

FIGURE 12. Spin density maps for thioimidoyls **21b**/**22b** and the corresponding transition states for β-fragmentation at the *S*-side [UB3LYP method, 6-311+G(d,p) basis set].

11.6−11.7 kcal/mol (see Table 3)] makes the two processes appear much more competitive than in reality.[38]

Conclusions

Thioimidoyl radicals were generated at low temperature by photolysis of dialkyl disulfides in the presence of alkyl isonitriles. Their EPR spectra showed hfs from H-atoms of the *N*-substituents, whereas no hfs from those of the *S*-substituents were resolved in any case. The low measured *g*-factors (2.0008−2.0014) are consistent with the idea that thioimidoyls are σ-radicals.

At higher temperatures the EPR spectra showed mainly the C-centered radical originally linked to the sulfur atom, as a result of β-fragmentation of the S−C bond of the thioimidoyl. Experiments carried out on unsymmetrical thioimidoyls showed that β-scission of the alkyl−N bond did not compete in any case. Calculation of the kinetic constants and Arrhenius parameters proved that the fragmentation is a fast process and practically every kind of C-centered radical can be efficiently produced by this route at $T \geq 20$ °C ($10^5 < k_f < 10^6$ s^{-1} at 298 K). Thermodynamic stabilization of the released radical plays, however, an important role: going from *S*-*n*-alkyl to *S*-*tert*-butyl causes a rate increase of ca. 2 orders of magnitude at 200 K, and release of resonance-stabilized radicals is so fast that the corresponding thioimidoyls could not be detected by EPR even at the lowest accessible temperatures.

The rate of S−C bond scission in thioimidoyls is ≥16 times the rate of O−C bond scission in oxyimidoyls at 200 K. The β-scission rate constants for selenoimidoyl radicals could not be estimated experimentally but they were computed by DFT calculations, which suggested that, within the imidoyl series, these radicals fragment with the lowest rate.

The competition between fragmentation and *5-exo* cyclization was studied by EPR experiments on two *S*-but-3-enyl-substituted thioimidoyl radicals. At 200 K the cyclization rates are higher than the β-scission rates, but the reverse is true at 300 K. It follows that for unsubstituted systems ring closure can be the major reaction channel only at low temperatures.

Computations on oxy-, thio-, and selenoimidoyls gave further support to the postulated bent, trans σ-structure of imidoyl radicals and reproduced well the observed selectivity for *S*-alkyl fragmentation with respect to *N*-alkyl scission, independent of the kind of the released alkyl radical. Calculations also showed that the fragmentation process preferentially occurs from the *s-cis* rotamer (X−C bond) of the imidoyl radical. Since thio- and selenoimidoyls prefer an *s-trans* conformation, for these radicals the actual scission pathway should therefore involve prior rotation of the X−C bond followed by fragmentation. The kinetic preference for scission through a non-W transition state was explained by comparison of the spin density maps in the imidoyl rotamers and in the corresponding transition states.

Experimental Section

Starting Materials. Cyclohexyl isonitrile, *tert*-butyl isonitrile, dibutyl disulfide, di-*iso*-propyl disulfide, di-*tert*-butyl disulfide, diallyl disulfide, dibenzyl disulfide, dibenzyl diselenide, cyclopentanethiol, methyl thioglycolate, 5-bromopent-3-yne, and *iso*-propyl bromide were obtained commercially. But-3-ene-1-thiol, di-(but-3-enyl) disulfide, 1-adamantyl isonitrile, and dodecane-1-isonitrile were prepared as described previously.[8] Dicyclopentyl disulfide[39] and dimethyl 2,2′-dithiodiacetate[40] were prepared from the corresponding thiols by oxidation with $KMnO_4/CuSO_4$ according to a reported procedure.[41]

EPR Spectra. EPR spectra were obtained with a Bruker EMX 10/12 spectrometer operating at 9.5 GHz with 100 kHz modulation. For reactions performed in cyclopropane (up to 0.5 mL), the solution was degassed on a vacuum line via the freeze−pump−thaw technique, and the tube was flame-sealed. In all cases where spectra were obtained, hfs were assigned with the aid of computer simulations using the Bruker Simfonia software package. For kinetic measurements, signals were double-integrated by use of the Bruker WinEPR software and radical concentrations were calculated by reference to a known concentration of DPPH, as described previously.

Thioacetic Acid *S*-Pent-2-ynyl Ester. To a stirred solution of potassium thioacetate (2.86 g, 25.0 mmol) in acetone (250 mL) was added 1-bromo-pent-2-yne (3.68 g, 25.0 mmol). The mixture was left stirring at room temperature for 12 h. The solution was first evaporated in vacuo to reduce the volume of the organic solvent and then partitioned between H_2O and CH_2Cl_2 (3×). The combined organic layers were dried over anhydrous magnesium sulfate and evaporated in vacuo.

(38) Computations on the *cis-cyclized* radical **11C** (see Supporting Information, page S32, right figure) indicated it is more stable by as much as 7.4 kcal/mol than the *trans* isomer and its computed hfs are in much better agreement with the experimental ones. Calculations therefore suggest that the cyclized radical observed by EPR could be *cis*- and not *trans*-**11C**. All the thioimidoyl radicals are more stable in their *trans* configurations, and the C=N double bonds are not directly involved in the ring closures. Hence, the formation of the *cis-cyclized* radical implies a *trans*−*cis* equilibration of the starting thioimidoyls, followed by thermodynamically controlled *5-exo* cyclizations. This explanation is also favored by the relatively high activation barrier for reopening of *cis*-**11C** (19.7 kcal/mol compared to 12.7 kcal/mol for reopening of *trans*-**11C**). *Trans*−*cis* isomerization of thioimidoyls can be in principle a viable process, since they are isoelectronic with vinyl radicals, which in turn are well-known to undergo fast *E*/*Z* equilibration [see for instance (a) Singer, L. A. *Selective Organic Transformations*; Thyagarajan, B. S., Ed.; Wiley: New York, 1972; Vol. 11, p 239. (b) Lui, M. S.; Soloway, S.; Wedegaetner, D. K.; Kampmeier, J. A. *J. Am. Chem. Soc.* **1971**, *93*, 3809]. Further studies on this topic are underway.

(39) Balavoine, G.; Barton, D. H. R.; Gref, A.; Lellouche, I. *Tetrahedron* **1992**, *48*, 1883.

(40) Stoodley, R. J.; Watson, N. S. *J. Chem. Soc., Perkin Trans. 1* **1974**, 252.

(41) Noureldin, N. A.; Caldwell, M.; Hendry, J.; Lee, D. G. *Synthesis* **1998**, 1587.

The crude product was purified by column chromatography on silica gel with diethyl ether/hexane (1:9) as eluant to give the target compound (2.60 g, 18.3 mmol, 73%) as a yellow oil. ^{1}H NMR ($CDCl_3$) δ 1.11 (3 H, t, J = 7.5 Hz), 2.18 (2 H, qt, J_q = 7.5 Hz, J_t = 2.4 Hz), 2.35 (3 H, s), 3.64 (2 H, t, J = 2.4 Hz); ^{13}C ($CDCl_3$) δ 13.11, 14.40, 18.89, 30.84, 74.28 (C), 85.43 (C), 195.14 (C).

Pent-2-yne-1-thiol. According to the literature,[42] the thioacetic acid *S*-pent-2-ynyl ester (1.42 g, 10.0 mmol) was dissolved in 20 mL of anhydrous tetrahydrofuran and added dropwise to a suspension of lithium aluminum hydride (0.38 g, 4 equiv) in 10 mL of anhydrous ether under a nitrogen atmosphere at 0 °C. The reaction mixture was stirred at ambient temperature for 30 min, and the excess lithium aluminum hydride was destroyed by careful addition of 10 mL of 1 N aqueous HCl. The ether layer was separated, dried over anhydrous magnesium sulfate, and evaporated in vacuo. The crude product was purified by column chromatography on silica gel with ethyl ether/hexane (1:9) as eluant to give the title thiol (0.88 g, 8.8 mmol, 88%) as a yellow oil. ^{1}H NMR ($CDCl_3$) δ 1.13 (3 H, t, J = 7.5 Hz), 1.96 (1 H, t, J = 7.2 Hz), 2.20 (2 H, qt, J_q = 7.5 Hz, J_t = 2.3 Hz), 3.27 (2 H, dt, J_d = 7.2 Hz, J_t = 2.3 Hz); ^{13}C ($CDCl_3$) δ 13.13, 13.46, 14.49, 38.61 (C), 85.19 (C).

Bis(penty-2-ynyl) Disulfide (5g). According to the literature,[41] the pent-2-yne-1-thiol (0.5 g, 5.0 mmol) was placed in a 100 mL round-bottomed flask and dissolved in CH_2Cl_2 (40 mL). A homogeneous mixture of $KMnO_4$ (1.0 g) and $CuSO_4$ (1.0 g) was added and the heterogeneous mixture was stirred at room temperature. The progress of the reaction was monitored by TLC until no thiol was detected. The contents of the flask were then filtered through Celite and washed with CH_2Cl_2 (2 × 20 mL) and Et_2O (2 × 20 mL). The combined organic layers were evaporated in vacuo and the crude product was purified by column chromatography on aluminum oxide with hexane as eluant to give the disulfide (0.29 g, 1.5 mmol, 59%) as a yellow sticky oil. ^{1}H NMR ($CDCl_3$) δ 1.14 (3 H, t, J = 7.4 Hz), 2.22 (2 H, qt, J_q = 7.4 Hz, J_t = 2.4 Hz), 3.60 (2 H, t, J = 2.4 Hz); ^{13}C ($CDCl_3$) δ 13.26, 14.41, 29.01, 75.33 (C), 87.11 (C).

Isopropyl Selenocyanate.[43] A solution of potassium selenocyanate (0.58 g, 4 mmol) in DMF (4 mL) under an argon-filled balloon was heated to 75 °C, and *i*-propyl bromide (0.49 g, 4 mmol) was added. The resulting mixture was stirred for 3 h at 75 °C. Potassium carbonate [0.55 g, 4 mmol in water (1.6 mL)] was slowly introduced by syringe. The resulting mixture was stirred for 3 h at 75 °C and then hydrolyzed (10 mL of water) and extracted with ether (2 × 20 mL). The ether fractions were combined, washed with water (2 × 20 mL), and dried over anhydrous magnesium sulfate. The solvent was evaporated in vacuo. The crude mixture was purified by column chromatography on silica gel with pentane as eluant to provide the target compound (0.41 g, 2.75 mmol, 69%) as a colorless oil. ^{1}H NMR δ 1.65 (6 H, d, J = 6.9 Hz), 3.74 (1 H, heptet, J = 6.9 Hz); ^{13}C NMR δ 25.5, 38.9, 102.1 (C).

Diisopropyl Diselenide (7b).[43] To isopropyl selenocyanate (0.41 g, 2.75 mmol) and ethanol (7 mL) under an argon-filled balloon was added sodium hydroxide (0.06 g, 1.38 mmol in 0.3 mL of water) by syringe. The resulting mixture was stirred for 0.5 h at ambient temperature and then hydrolyzed (10 mL of water) and extracted with ether (2 × 20 mL). The ether fractions were combined, washed with water (2 × 20 mL), and dried over anhydrous magnesium sulfate. The solvent was evaporated in vacuo. The crude mixture was fractionated by column chromatography on silica gel with pentane as eluant to provide the diselenide (0.39 g, 1.60 mmol, 58%) as an intense yellow oil. ^{1}H NMR δ 1.44 (12 H, d, J = 6.7 Hz), 3.24 (2 H, heptet, J = 6.7 Hz).

Photochemical Reaction of Dibenzyl Diselenide with *t*-Butyl Isonitrile. The diselenide **7f** (ca. 15 mg) and *tert*-butyl isonitrile (15 mg) were dissolved in benzene (0.5 mL) and photolyzed at ambient temperature for 4 h with light from a 400 W medium-pressure Hg lamp. The solvent was evaporated and the mixture was analyzed by GC−MS. Peak 134, *t*-butyl isoselenocyanate (**9**), *m*/*z* (%) 165 (6), 163 (39), 161 (18), 160 (5) 159 (6), 148 (3), 107 (3), 57 (100); peak 385, dibenzyl (main product), *m*/*z* (%) 182 (M^+, 83), 92 (7), 91 (100), 65 (14), together with minor unidentified products.

Photochemical Reaction of Diisopropyl Diselenide with *t*-Butyl Isonitrile. The diselenide (ca. 15 mg) and *tert*-butyl isonitrile (15 mg) were dissolved in benzene (0.5 mL) and photolyzed at ambient temperature for 4 h with light from a 400 W medium-pressure Hg lamp. The solvent was evaporated and the mixture was analyzed by GC−MS. Peak 139, *tert*-butyl isoselenocyanate (**9**).

Photochemical Reaction of Dibut-3-enyl Disulfide with *t*-Butyl Isonitrile. The disulfide (**5i**) (ca. 10 mg) and *tert*-butyl isonitrile (ca. 10 mg) in a 4 mm o.d. quartz tube were degassed on a vacuum line and dissolved in cyclopropane (ca. 0.5 mL). The tube was flame-sealed and photolyzed at 0 °C with UV light from a 500 W super-pressure Hg arc lamp for 1 h. The tube was opened at low temperature, the cyclopropane was carefully evaporated, and the contents were dissolved in $CDCl_3$. The ^{1}H NMR showed unreacted starting materials overlapping a complex sequence of product signals. GC−MS analysis also showed starting materials and indicated the following products (yields are given as % of total products): peak 94, *t*-butyl isothiocyanate (17.3%), *m*/*z* (%) 115 (M^+, 92), 100 (23), 72 (10), 57 (100); peak 191, dibut-3-enyl sulfide (3.6%), *m*/*z* (%) 142 (M^+, 7), 114 (11), 101 (55), 88 (56), 85 (23), 73 (15), 67 (80), 59 (58), 55 (100); peak 253, *tert*-butyl-(3-methyldihydrothiophen-2-ylidene)amine **14C** (14.3%), *m*/*z* (%) 171 (M^+, 27), 156 (35), 143 (8), 116 (12), 87 (8), 68 (10), 57 (100), 56 (19); peak 259, probably *tert*-butyl-(tetrahydrothiopyran-2-ylidene)amine **16C** (0.4%), *m*/*z* (%) 171 (M^+, 8), 156 (23), 142 (100), 127 (32), 113 (9), 108 (28), 99 (64), 79 (16), 67 (53), 57 (44); peak 280, *tert*-butyl-(3-methylenedihydrothiophen-2-ylidene)amine **15C** (11.3%), *m*/*z* (%) 169 (27), 154 (22), 113 (13), 67 (8), 57 (100); peak 356, probably *N*-*tert*-butyl-thioformimidic acid but-3-enyl ester **17C** (7.0%), *m*/*z* (%) 171 (M^+, 7), 170 (9), 138 (14), 115 (4), 82 (13), 57 (100); peak 401, *tert*-butyl-(3-pent-4-enyldihydrothiophen-2-ylidene)amine **13C** (23.9%), *m*/*z* (%) 225 (M^+, 3), 210 (12), 170 (11), 157 (77), 114 (12), 101 (28), 57 (100); peak 494, 3-(but-3-enylsulfanylmethyldihydrothiophen-2-ylidene)-*tert*-butylamine **19C** (4.4%), *m*/*z* (%) 257 (M^+, 9), 202 (27), 170 (11), 156 (29), 146 (60), 114 (33), 100 (12), 87 (17), 57 (100), 55 (31); peak 526, probably the dimer **18C** (2.6%), *m*/*z* (%) 170 (58), 114 (31), 57 (100), 55 (27); peak 640, probably the product from cross-coupling radicals **6C** and **11C** (5.9%), *m*/*z* (%) 283 (8), 227 (9), 184 (30), 183 (100), 170 (29), 157 (55), 127 (19), 114 (15), 101 (22), 57 (96); several minor unidentified components were also present (ca. 8% total). Butene, butane, and octa-1,7-diene were not detected, probably because their volatility caused their escape during solvent removal.

Photochemical Reaction of Dibut-3-enyl Disulfide with Adamantane- 1-isonitrile. The disulfide (**5i**) (ca. 10 mg) and adamantane-1-isonitrile (ca. 10 mg) in a 4 mm o.d. quartz tube were degassed on a vacuum line and dissolved in cyclopropane (ca. 0.5 mL). The tube was flame-sealed and photolyzed at 0 °C with UV light from a 500 W super-pressure Hg arc lamp for 1 h. The tube was opened at low temperature, the cyclopropane was carefully evaporated, and the contents were dissolved in $CDCl_3$. The ^{1}H NMR showed unreacted starting materials overlapping a complex sequence of products. GC−MS analysis also showed starting materials and indicated the following products: peak 433, adamantane-1-isothiocyanate, *m*/*z* (%) 193 (M^+, 7), 135 (100), 93 (11), 79 (8); peak 541,

(42) Yang, X. F.; Mague, J. T.; Li, C. J. *J. Org. Chem.* **2001**, *66*, 739.

(43) (a) Krief, A.; Dumont, W.; Delmotte, C. *Angew. Chem., Int. Ed.* **2000**, *39*, 1669. (b) Krief, A.; Dumont, W.; Delmotte, C. *Tetrahedron* **1997**, *53*, 12147.

probably *N*-(1-adamantyl)-thioformimidic acid but-3-enyl ester **17D**, *m*/*z* (%) 249 (M^+, 10), 192 (3), 135 (100); several additional unidentified peaks were also present.

Acknowledgment. We thank the Royal Society of Chemistry, St. Andrews University, MIUR (2002−2003 Funds for "Radical Processes in Chemistry and Biology: Fundamental Aspects and Applications in Environment and Material Science"), and the University of Bologna (2001−2003 Funds for Selected Research Topics) for financial support. We also thank Dr. B. Maillard (Bordeaux) for providing samples of diallyl and di-*i*-propyl disulfide and Dr. M. Guerra (ISOF-CNR, Bologna) for helpful discussions on theoretical calculations.

Supporting Information Available: (i) General experimental procedures; (ii) EPR spectra of imidoyl radicals **6Aa**−**d**, **6Ba**−**c**, **6Ca**−**d,i**, **6Da**−**d,i**, *n*-$C_{12}H_{25}NC^{\bullet}O$-*t*-Bu, and *c*-$C_6H_{11}NC^{\bullet}O$-*t*-Bu; (iii) variable-temperature EPR spectra for fragmentations of imidoyl radicals **6Aa**−**d**, **6Ba,b**, **6Ca**−**d**, **6Da**−**c**, *n*-$C_{12}H_{25}NC^{\bullet}O$-*t*-Bu, and *c*-$C_6H_{11}NC^{\bullet}O$-*t*-Bu; (iv) Arrhenius plots and equations for fragmentations of imidoyls **6Aa**−**d**, **6Ba,b**, **6Ca**−**d,g**, **6Da**−**c**, *n*-$C_{12}H_{25}NC^{\bullet}O$-*t*-Bu (both scission and k_a/k_H), and *c*-$C_6H_{11}NC^{\bullet}O$-*t*-Bu; (v) spin densities and hfs of imidoyl radicals **21a**−**c** and **22a**−**c**; (vi) computed structures (and hfs) of radicals **6Ci**, **11C**, and the connecting transition state; (vii) Cartesian coordinates of radicals **6Fk**, **6Gb**, **6Cc**, **21a**−**c**, **22a**−**c**, **6Ci**, **11C**, and the transition states related to their reactions; and (viii) ^1H and ^{13}C NMR spectra of thioacetic acid *S*-pent-2-ynyl ester, pent-2-yne-1-thiol, and disulfide **5g**. This material is available free of charge via the Internet at http://pubs.acs.org.

JO0353637